Annals of Nuclear Medicine Vol. 19, No. 6, 425–433, 2005

Use of reference tissue models for quantification of histamine H_1 receptors in human brain by using positron emission tomography and [^{11}C]doxepin

Atsuro SUZUKI,* Manabu TASHIRO,** Yuichi KIMURA,*** Hideki MOCHIZUKI,**** Kenji ISHII,*** Hiroshi WATABE,***** Kazuhiko YANAI,**** Kiichi ISHIWATA*** and Keizo ISHII*

*Department of Quantum Science and Energy Engineering, Tohoku University
**Cyclotron and Radioisotope Center, Tohoku University
***Positron Medical Center, Tokyo Metropolitan Institute of Gerontology
****Department of Pharmacology, Tohoku University School of Medicine
*****Department of Investigative Radiology, Research Institute, National Cardiovascular Center

The aim of the present study is to evaluate the validity of the simplified reference tissue model (SRTM) and of Logan graphical analysis with reference tissue (LGAR) for quantification of histamine H_1 receptors (H1Rs) by using positron emission tomography (PET) with [^{11}C]doxepin. These model-based analytic methods (SRTM and LGAR) are compared to Logan graphical analysis (LGA) and to the one-tissue model (1TM), using complete datasets obtained from 5 healthy volunteers. Since H1R concentration in the cerebellum can be regarded as negligibly small, the cerebellum was selected as the reference tissue in the present study. The comparison of binding potential (*BP*) values estimated by LGAR and 1TM showed good agreement; on the other hand, SRTM turned out to be unstable concerning parameter estimation in several regions of the brain. By including the results of noise analysis, LGAR became a reliable method for parameter estimation of [^{11}C]doxepin data in the cortical regions.

Key words: model-based analysis, histamine H_1 receptor, [^{11}C]doxepin, PET

INTRODUCTION

THE HISTAMINERGIC NEURON SYSTEM in the brain plays important roles in various physiological functions such as wakefulness, cognition and memory.[1–3] These brain functions are mediated mainly by histamine H_1 receptors (H1Rs), one of 4 known subtypes (H_1, H_2, H_3, and H_4).[1] For mapping the distribution of H1Rs in the human brain, positron emission tomography (PET) has been used with [^{11}C]-labeled doxepin, a potent H1R antagonist.[4] [^{11}C]doxepin is radiotracer of choice because of its high affinity to H1Rs and its ability to penetrate the blood-brain barrier.[5] PET with [^{11}C]doxepin has been applied to the investigation of various pathological states including Alzheimer's disease and epilepsy,[6,7] as well as sedation due to antihistamines observed in patients with various disorders.[2,8–10]

In most H1R mapping studies, the binding potential (*BP*) of [^{11}C]doxepin to H1Rs is calculated using the graphical method introduced by Logan and colleages.[11] As part of our recent efforts to establish a suitable analytical method for [^{11}C]doxepin, we first demonstrated that the one-tissue model (1TM) was more stable in parameter estimation of [^{11}C]doxepin kinetics than the two-tissue model (2TM) which leads to a large variation in parameter values, depending strongly upon the startup parameters.[12] Thereafter, we also developed a short (15-min-long) static scan protocol of one-point blood sampling to reduce physical and psychological stress of test persons in clinical trials, in which the persons are to be scanned 3 to 4 times.[13] So far, we have not examined the possible application of reference tissue models to [^{11}C]doxepin data, where blood sampling is not needed. Two major reference tissue models are available: the simplified reference tissue model (SRTM)[14] and Logan graphical analysis with

Received November 15, 2004, revision accepted March 16, 2005.

For reprint contact: Keizo Ishii, D.Sci., Department of Quantum Science and Energy Engineering, Tohoku University, Aramaki-aza-aoba 01, Aoba-ku, Sendai 980–8579, JAPAN.
E-mail: keizo.ishii@qse.tohoku.ac.jp

reference tissue (LGAR).[15]

A compartment model for receptor analysis should be developed based on the kinetic tracer behavior in target organs. Usually, this behavior is described with a three-compartment model (two-tissue model: 2TM),[16] but if rapid equilibrium occurs among free, nonspecifically and specifically bound compartments, a 1TM is suitable for the kinetic analysis.[17] In fact, our previous study already demonstrated that 1TM was suitable for describing the kinetic data of [^{11}C]doxepin whereas the results based on 2TM highly depended on initial parameter estimation so that different initial values produced different results.[12] Therefore, 2TM was excluded from the present evaluation. In the present study, H1R-[^{11}C]doxepin binding parameters estimated by 2 reference tissue models, SRTM and LGAR, were compared to those calculated by LGA and by 1TM. Reliability of these analytical methods was also examined by comparing the obtained parameters to those calculated by 1TM, probably the most reliable method in the present evaluation.

MATERIALS AND METHODS

Subjects

Five healthy male volunteers, 21–27 years old, participated in the present study. None had any previous history of psychiatric or neurological disorders and none of them showed anatomical abnormalities in brain MRI images. Written informed consent was obtained from every subject before enrollment in the present study. The volunteers were asked to abstain from taking medication for a week before the study, and from taking tobacco, alcohol and caffeine on the day of experiment. The study was approved by the respective ethics committees of the Tokyo Metropolitan Institute of Gerontology and of Tohoku University Graduate School of Medicine, and was performed in compliance with relevant laws.

PET measurement

Dynamic scans in two-dimensional mode were performed using Headtome-V (Shimadzu Co., Kyoto, Japan) with 63 slices of 128-by-128 voxels each at transverse resolution of 4.5 mm full width of half maximum (FWHM) and at axial resolution of 5.8 mm FWHM. PET images were reconstructed with a filtered backprojection algorithm, and corrections were applied for dead time, detector uniformity and photon attenuation. The frame arrangement was 10 sec × 6 frames, 30 sec × 3 frames, 60 sec × 5 frames, 2.5 min × 5 frames and 5 min × 14 frames for a total of 90 minutes and [^{11}C]doxepin was prepared as previously described.[12] The injected radioactivity dose of [^{11}C]doxepin was 493 ± 109 MBq and the cold mass was 23 ± 16 nmol (mean ± SD). Arterial blood was sampled every 10 sec for the first 150 sec post-injection and afterwards at 3, 5, 7, 10, 15, 20, 30, 40, 50, 60, 75 and 90 min. Metabolite analysis was carried out using 6 plasma samples obtained 3, 10, 20, 30, 40 and 60 min after the injection as previously described.[12]

Model-based analysis

The 2TM provides a general framework for model-based analysis that consists of a plasma compartment (C_p) and two-tissue compartments: one compartment is for the free and nonspecifically bound ligands (C_{f+ns}), and the other is for the specifically bound ligands (C_s). The transfer of the ligand across compartments is governed by 4 fractional rate constants, K_1, k_2, k_3 and k_4, where K_1 is the influx rate constant into C_{f+ns}, k_2 is the efflux rate constant from C_{f+ns}, k_3 is the association rate constant into C_s, and k_4 is the dissociation rate constant from C_s, respectively. If the association and dissociation rates between free ligands and receptors are sufficiently rapid compared to the transport parameters K_1 and k_2, the model can be simplified using a one-tissue compartment, where all of the free ligands and nonspecifically and specifically bound ligands are represented by a single tissue compartment. This model is the 1TM,[17] where the concentration time function $C_T(t)$ in a certain regional tissue is expressed as follows,

$$C_T(t) = K_1 C_P(t) \otimes e^{-k_{2a}t} \quad (1)$$

where $C_P(t)$ is the concentration time function in the plasma, and k_{2a} is the efflux rate constant from the single tissue compartment. The distribution volume (DV) can be written as $DV = K_1/k_{2a} = K_1/k_2\,(1 + k_3/k_4)$. Provided that the H1R concentration in the reference tissue is negligibly small and that K_1/k_2 is constant in the all brain regions, the binding potential ($BP = k_3/k_4$) can be obtained as $BP = DV/DV^{REF} - 1$, where DV^{REF} is DV in the reference tissue. In the present study, the cerebellum was used as the reference tissue because of the negligibly small H1R concentration in this region.

In SRTM,[14] the target and reference tissues are described as a one-tissue model. If K_1/k_2 is constant in the all brain regions, $C_T(t)$ in the tissue is expressed as follows,

$$C_T(t) = R_1 C_R(t) + \left\{ k_2 - \frac{R_1 k_2}{1 + k_3/k_4} \right\} C_R(t) \otimes e^{-k_2/(1+k_3/k_4)t} \quad (2)$$

where $C_R(t)$ is the concentration time function in the reference region, and R_1 is the ratio of delivery to the regional tissue compared to the reference region (ratio of influx). This method can avoid the complexity of arterial blood sampling.

The formula for LGA is expressed as follows:[11]

$$\frac{\int_0^T C_T(t)dt}{C_T(T)} = DV \frac{\int_0^T C_P(t)dt}{C_T(T)} + a_1 \quad (3)$$

where the values of the slope DV and the intercept a_1 are obtained by linear regression. The BP value is obtained as $BP = DV/DV^{REF} - 1$. LGAR[15] is expressed as follows:

$$\frac{\int_0^T C_T(t)dt}{C_T(T)} = DVR\left(\frac{\int_0^T C_R(t)dt + C_R(t)/k_2'}{C_T(T)}\right) + a_2 \quad (4)$$

where DVR is the distribution volume ratio (DV/DV^{REF}), a_2 is an intercept term, and k_2' is an average value in the reference tissue. Then BP is obtained as $BP = DVR - 1$, and the complexity of arterial blood sampling is avoided.

Data analysis

Regions of interest (ROIs) were drawn on 5 cortical structures (the frontal, temporal, occipital, parietal and cingulate cortices) bilaterally, 3 subcortical structures (the thalamus, caudate nucleus and putamen) bilaterally, and on the midbrain centrally. Two ROIs in right and left regions were drawn on cortical and subcortical structures. In results, 17 ROI data were obtained to obtain averaged tissue time-activity curves (tTACs) as reported previously.[12] One additional ROI was drawn on the cerebellum to obtain an averaged tTAC in the reference tissue.

In 1TM and SRTM analysis, parameters were estimated in standard nonlinear fitting algorithms of the Gauss-Newton type. The nonlinear regression was considered to have converged if all parameters had been changed by less than 0.1% from the previous iteration. Failure of convergence was declared if nonlinear regression failed to reach convergence after 100 iterations, and if the determinant of the normal equation's coefficient matrix was less than 10^{-20}. The initial values of K_1 and k_2 in 1TM were 0.5 [ml/g/min] and 0.02 [/min], respectively, and those of R_1, k_2 and BP in SRTM were 1, 0.01 [/min] and 0.5, respectively. Delay between tTAC and the plasma time-activity curve (pTAC) was estimated using an averaged tTAC of the whole-brain. In the present study, cerebral blood volume was disregarded because it is generally small (3–5%).[18]

BP values derived from different methods were compared in terms of the following criteria: 1) failure rate, 2) physiological rationality, and 3) sensitivity to noise.

1) Failure rate

In general, a failure in parameter estimation occurs in the following cases: a) when the nonlinear regression procedure fails to reach convergence, b) when the estimated parameter is unstable against variation of the initial parameter values in nonlinear regression, c) when BP values calculated by $DVR - 1$ become negative, d) when the standard error in the estimated parameter becomes very large. Note that the standard error here means the error in a parameter caused by the inherent uncertainty of this estimation procedure. The standard error of the parameter was obtained from the diagonal of the covariance matrix, and the result of parameter estimation was defined as "failure" when the standard error exceeded 30%.[19] In the present analysis, a total of 85 ROIs (17 ROIs from each of 5 subjects) were examined. Then, the failure rate of each modeling procedure was expressed as [number of regions whose estimation failed]/85 × 100%.

2) Physiological rationality

Physiological rationality was assessed by comparing the estimated BP values to H1R densities measured in the brain *in vitro* using [^{3}H]doxepin, as reported by Kanba and Richelson.[20] In addition, correlations were examined between BP values calculated by 1TM and those by the other methods using Pearson's correlation test.

3) Sensitivity to noise

Simulation was performed to evaluate the sensitivity to noise for each model-based method. This evaluation was carried out for BP estimation for the temporal cortex that was rich in H1Rs and in the occipital cortex that was relatively poor in H1Rs, by using the cerebellum as the reference region. Simulation data (ROI_N) are expressed as the following:

$$ROI_N(t) = ROI(t) + SD(t) \times N(0,1) \quad (5)$$

$$SD(t) = \sqrt{\frac{c \times ROI(t) \times e^{\lambda t}}{\Delta t}}$$

where a non-dimensional constant c determines the noise level, λ is a decay constant of the isotope, Δt is frame length, $N(0,1)$ is a pseudo-random number of a Gauss distribution with zero mean and standard deviation of one.[21]

In the present simulation, random noise was introduced and noisy datasets were analyzed with SRTM, LGAR, LGA and 1TM, at 8 different noise levels (noise level c = 5, 10, 15, 20, 25, 30, 35, 40). The noise levels of the actual brain image data were considered to remain within the range of the noise levels mentioned above. In the present simulation analysis, 1000 different curves were generated for each noise level, and the effects of noise levels on the results were evaluated using a bias, i.e. the difference between the true BP values and BP values obtained in 1000 simulations, for each modeling method.

Simulation on the effect of nonspecific binding

In order to investigate the effect of nonspecific binding on the parameter estimation, another simulation was performed according to the following procedure. Simulated tTACs in the various cortical regions and the reference tissue (the cerebellum) were generated by 1TM with varying nonspecific binding values of DV^{REF} = 5, 10, 15, 20, 25, 30. Based on an assumption that nonspecific binding is equal in the target and reference regions, DV^{REF} was set to be identical to the nonspecific binding in the target regions in this simulation analysis. Based on the results of ROI analysis in the temporal cortex, the parameters K_1 and DV^{ROI} in the ROI were fixed at 0.495 [ml/g/min] and 36.5, respectively where DV^{ROI} represented the

Table 1 Calculated binding potential (*BP*) values using simplified reference tissue model (SRTM), Logan graphical analysis with reference tissue (LGAR), Logan graphical analysis (LGA) and one-tissue model (1TM), compared to histamine H_1 receptor (H1R) density in autopsied human brains.[20] In the frontal, temporal, occipital, parietal, and cingulate cortices, thalamus, caudate nucleus and putamen, mean ± SD of 10 ROIs (two ROIs in right and left regions for each of 5 subjects). In the midbrain, mean ± SD of 5 ROIs (one ROI for each of 5 subjects)

Brain areas	Estimated binding potential								H1R density measured *in vitro* (fmol/mg protein/0.1 nM)
	SRTM		LGAR		LGA		1TM		
	mean	%SD	mean	%SD	mean	%SD	mean	%SD	
frontal cortex	0.53	26	0.36	18	0.38	24	0.37	25	19.1
temporal cortex	0.51	14	0.47	16	0.49	25	0.49	24	23.5
parietal cortex	0.2	29	0.36	20	0.37	26	0.37	25	16.6
occipital cortex	0.35	34	0.24	21	0.25	19	0.25	16	13.2
cingulate cortex	—	—	0.39	19	0.39	20	0.4	21	22.3
thalamus	0.24	19	0.31	17	0.31	16	0.34	16	4.3
caudate nucleus	0.32	16	0.23	44	0.24	48	0.28	44	5.3
putamen	0.32	14	0.34	29	0.34	29	0.36	27	4.4
midbrain	—	—	0.16	146	0.22	110	0.14	148	2.2

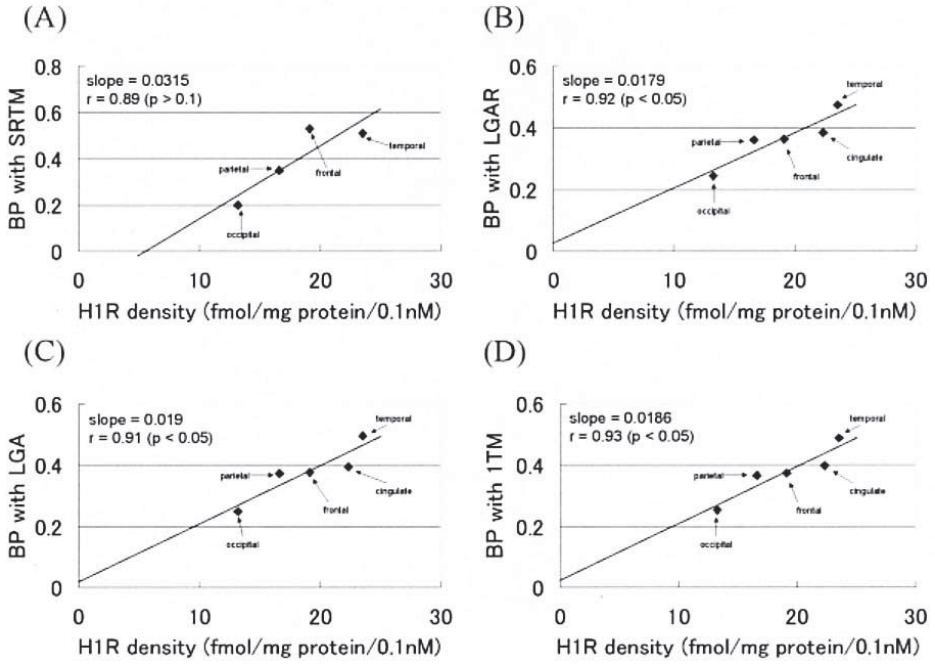

Fig. 1 Relationship between binding potential (*BP*) values and histamine H_1 receptor (H1R) densities in autopsied human brains.[20] The simplified reference tissue model (SRTM) (A), Logan graphical method with reference tissue (LGAR) (B), Logan graphical method with arterial sampling (LGA) (C), and one tissue model (1TM) (D).

sum of distribution volumes containing both nonspecific and specific bindings. The true *BP* values were calculated as $BP = DV^{ROI}/DV^{REF} - 1$. Since the DV^{ROI} value was fixed at 36.5 and DV^{REF} values were set to be changeable, high DV^{REF} values would result in low *BP* values. The parameter K_1 in the reference tissue was fixed at 0.529 [ml/g/min]. Random noise was introduced (noise level: $c = 15$) to the dynamic image data, and the noisy tTACs were analyzed with SRTM, LGAR, LGA and 1TM modeling methods at different DV^{REF} values, for which 1000 realizations of noisy tTACs were generated. Finally, the effect of nonspecific binding in the target and reference regions was evaluated by comparing *BP* estimates with the truth.

RESULTS

In the present study, *BP* values were calculated from *DV* or *DVR* values determined by each model using ROI-derived tTACs, and these *BP* values were then compared.

The mean cerebellar k_2 (0.022 [/min]) obtained by 1TM was used in LGAR. The averaged starting times t_0 for linear regression were 4.7 ± 1.7 [min] and 4.6 ± 1.8 [min] for LGA and LGAR, respectively.

Failure rate

Mean *BP* values estimated by SRTM, LGAR, LGA, and 1TM across the 5 subjects are presented in Table 1. In parameter estimation, 1TM produced reasonable *BP* values in all of 85 ROIs studied (failure rate = 0%), and LGA failed in 2 out of 85 ROIs (failure rate = 2.4%), respectively. SRTM, however, failed in 58 out of 85 ROIs (failure rate = 68.2%), while LGAR failed in only 1 out of 85 ROIs (failure rate = 1.2%).

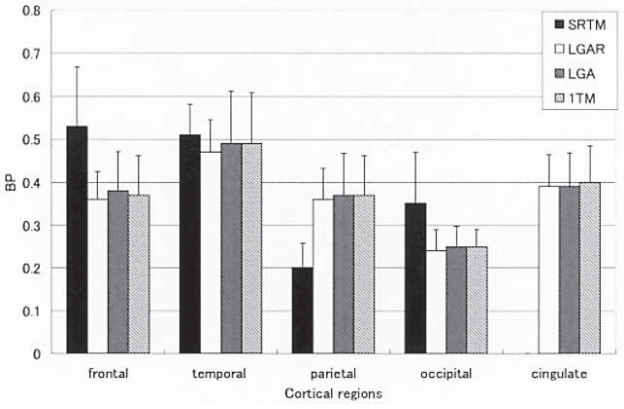

Fig. 2 Calculated binding potential (*BP*) values using simplified reference tissue model (SRTM), Logan graphical analysis with reference tissue (LGAR), Logan graphical analysis (LGA) and one-tissue model (1TM) in the five cortical regions (frontal, temporal, occipital, parietal and cingulate cortices). The *BP* value in the cingulate cortex was not available with SRTM.

Physiological rationality and correlation to results of 1TM

H1R densities in the human brain measured *in vitro* using [^{3}H]doxepin as a radioligand are given in Table 1.[20] H1R densities in the subcortical regions were lower than a quarter of the highest density in the cortex. However, a marked discrepancy in cortical/subcortical ratios was seen between the *BP* values measured *in vivo* and H1R densities measured *in vitro*. And the correlation between H1R densities and *BP* values was not statistically significant ($p > 0.05$) in the subcortical regions or in the midbrain for all of the 4 methods such as SRTM, LGAR, LGA and 1TM. Correlation of H1R densities to the *BP* values was statistically significant in the cortical regions such as the frontal, temporal, occipital, parietal and cingulate cortices, and the correlation coefficients were $r = 0.89$ ($p > 0.1$), $r = 0.92$ ($p < 0.05$), $r = 0.91$ ($p < 0.05$) and $r = 0.93$ ($p < 0.05$), respectively (Fig. 1).

In Figure 2, *BP* values in the 5 cortical regions are shown. Further correlation analysis demonstrated significant correlations of the BP values based on 1TM to those estimated by SRTM ($r = 0.73$: $p < 0.001$), LGAR ($r = 0.94$: $p < 0.001$) and by LGA ($r = 0.99$: $p < 0.001$), respectively

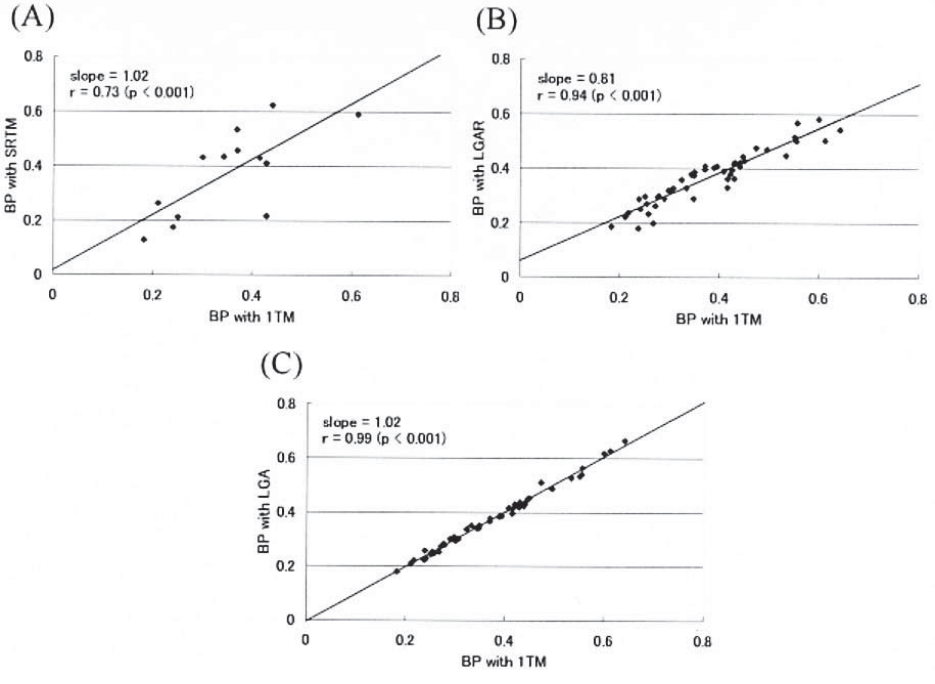

Fig. 3 Correlations between binding potential (*BP*) values calculated by 1TM and other three methods: the simplified reference tissue model (SRTM) (A), Logan graphical method with reference tissue (LGAR) (B), and Logan graphical method with arterial sampling (LGA) (C).

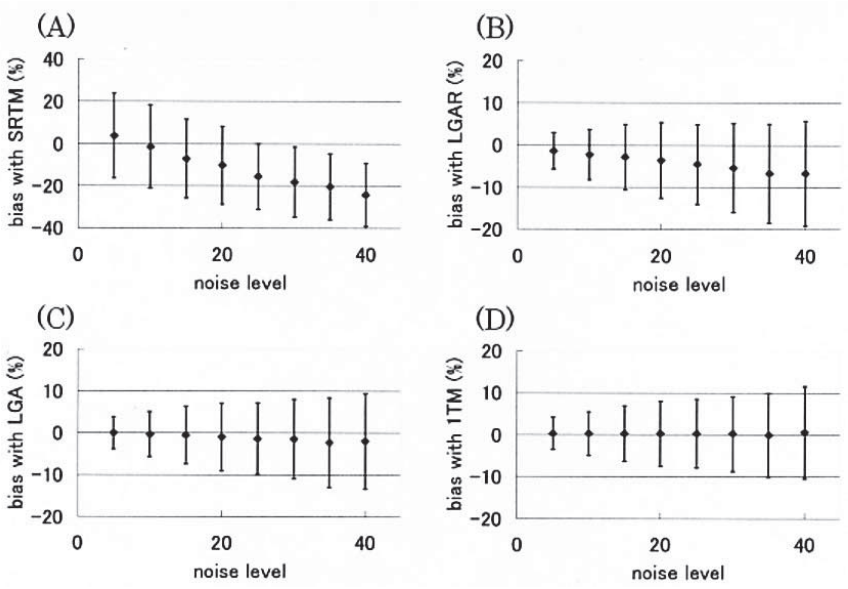

Fig. 4 Results of noise analysis in *BP* estimation in the temporal cortex with the simplified reference tissue model (SRTM) (A), Logan graphical method with reference tissue (LGAR) (B), Logan graphical method with arterial sampling (LGA) (C), and one tissue model (1TM) (D). The bias is between binding potential (*BP*) values averaged over 1000 simulations and the true *BP*. Noise level is described in MATERIALS AND METHODS section.

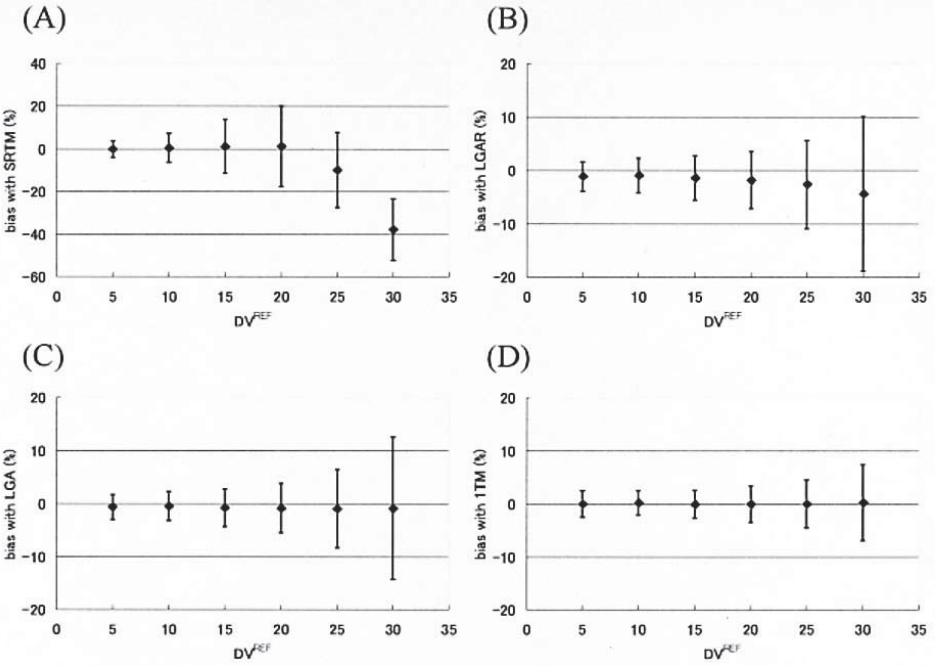

Fig. 5 Results of simulation in *BP* estimation at different DV^{REF}. The simplified reference tissue model (SRTM) (A), Logan graphical method with reference tissue (LGAR) (B), Logan graphical method with arterial sampling (LGA) (C), and one tissue model (1TM) (D). The bias is between binding potential (*BP*) values averaged over 1000 simulations and the true *BP*. Noise level *c* was fixed at 15.

(Fig. 3). The mean biases from the *BP* value based on 1TM (standard) in the cortical regions (50 ROIs: 10 ROIs for each of 5 subjects) were 6.5% with SRTM, 1.3% with LGAR and 0.3% with LGA, respectively.

Sensitivity to noise

The effect of noise in dynamic images on resultant *BP* values was examined for SRTM, LGAR, LGA and 1TM using simulation analysis. Simulated datasets were gener-

ated using TACs in the cerebellum (1TM, $K_1 = 0.529$ [ml/g/min], $k_2 = 0.0220$ [/min]), in the temporal cortex (1TM, $K_1 = 0.495$ [ml/g/min], $k_2 = 0.0140$ [/min]) and in the occipital cortex (1TM, $K_1 = 0.461$ [ml/g/min], $k_2 = 0.0153$ [/min]). Figure 4 shows results of the simulation for *BP* estimation in the temporal cortex. At all the noise levels studied here, the mean bias of *BP* values in 1TM was demonstrated to be smaller than in those of SRTM, LGAR and in LGA for both the temporal and the occipital cortices.

Simulation study on nonspecific binding

Figure 5 shows the results of simulation concerning *BP* estimation at different DV^{REF} values. As to the parameter estimation based on 1TM, biases were very small at all DV^{REF} values. In contrast, a trend toward an increased bias was observed with higher DV^{REF} values for LGA, LGAR and SRTM. Particularly, biases of SRTM at high DV^{REF} values were the largest among the all the methods examined. The results indicated that the failure rate of SRTM clearly increased with increased DV^{REF} values (for instance, 20, 25 and 30) ranging from 1.9, 28.0 to 66.5%, respectively, though the failure rate remained 0% when the DV^{REF} was smaller than 15. On the other hand, failure rates of 1TM, LGA and LGAR were always 0% at all given DV^{REF} values.

DISCUSSION

In the present study, the authors examined *BP* values estimated by SRTM and LGAR in terms of parameter stability and of correlation between autopsy data and *BP* values estimated by 1TM. An analytical method requiring arterial blood sampling is most accurate as the minimum bias and the highest correlation coefficients appear in the comparison of 1TM and LGA. However, it is difficult to apply this method to subjects in some situations such as in the presence of blood-borne infections.[15] Using reference tissue models, blood sampling and time-consuming metabolite measurements can be avoided and scanning protocol and data analysis can be simplified.[14]

Simplified reference tissue model (SRTM)

This method has been widely accepted and used for various tracers; however, this method was demonstrated to be unstable in parameter estimation of [^{11}C]doxepin binding. The failure rate of SRTM was so high (68.2%) that parameters were not available in many brain regions. The parameter correlation to 1TM was fairly low ($r = 0.71$: $p < 0.001$) and its correlation to autopsy data was not significant ($r = 0.89$: $p > 0.1$). The authors additionally tested the linear estimation method employed in Gunn's implementation of SRTM.[22] This method also failed to obtain *BP* values in 16 out of 85 ROIs (failure rate = 18.8%) even when the criterion 4 (standard error of the estimated parameter larger than 30%) was not applied. A possible reason for the high failure rate in parameter estimation with SRTM might be due to the relatively high nonspecific binding that resulted in a relatively large *DV* value in the cerebellum, which exceeded a half of the cortical *DV* values[5,12] (Table 2). Since *DV* values represent total binding, the cerebellar *DV* includes nonspecific binding while the cortical *DV* includes both specific and nonspecific bindings. Even if the amount of nonspecific binding is equal in the cortex and the cerebellum as described previously,[12] relatively high nonspecific binding might obscure the signals of specific binding in the cortex. According to Jensen and colleagues, SRTM seemed to be unsuitable for kinetic analysis for the binding of a serotonin transporter antagonist, [^{11}C]-NS 4194, because of its high nonspecific binding throughout the brain.[23]

Table 2 Calculated distribution volume (*DV*) values using Logan graphical analysis (LGA) and one-tissue model (1TM)

Brain areas	Present study *DV*			
	LGA		1TM	
	mean	%SD	mean	%SD
frontal cortex	33.6	19.4	33.6	19.7
temporal cortex	36.5	20.5	36.4	20.0
parietal cortex	33.5	18.9	33.4	19.2
occipital cortex	30.4	15.9	30.5	15.9
cingulate cortex	33.9	16.7	34.1	17.1
thalamus	32.0	16.1	32.5	15.3
caudate nucleus	30.3	20.6	31.4	21.3
putamen	32.7	19.4	33.2	19.3
midbrain	27.1	15.2	27.4	15.3
cerebellum	24.3	15.6	24.3	15.6

Thus, an additional simulation analysis was conducted in the present study in order to investigate the effect of nonspecific binding on the results of parameter estimation. The simulation analysis demonstrated that high nonspecific binding was associated with a high failure rate due to a large error in parameter estimation with SRTM, even when all required assumptions were fulfilled for the use of this model. The high failure rate due to high nonspecific binding can be predicted by the equation (2), where the high nonspecific binding reflects low k_2 values. Suppose the k_2 value is extremely low, the first term in the right-hand side is dominant and the right-hand side is almost independent of the second term which contains *BP*, k_2 and R_1. This would be one of the reasons parameters cannot be estimated uniquely. The mean k_2 value measured for [^{11}C]doxepin in the cerebellum was low ($k_2 = 0.022$ [/min]) as compared with that of other neuroreceptor radioligands such as the D_2-receptor antagonist [^{11}C]raclopride (0.163 [/min]) and the D_1-receptor antagonist [^{11}C]SCH23390 (0.101 [/min]).[24] Generally, SRTM appears to be suitable for tracers with negligibly low nonspecific binding in the reference tissues such as [^{11}C]raclopride and [^{11}C]SCH23390, but is not suitable for tracers with relatively high nonspecific binding

throughout the brain such as [^{11}C]doxepin.[14]

Logan graphical analysis with reference tissue (LGAR)
This method[15] was introduced as an extended version of LGA[11] where tracer binding was evaluated as *DVR*. However, in order to calculate *BP* values expressed by *DVR* – 1, the two following assumptions are required.

The first assumption is that the region used as the reference is devoid of specific binding. Blocking studies showed that there is no appreciable difference in [^{11}C]doxepin binding in the cerebellum with or without administration of *d*-chlorpheniramine, a highly potent H1R antagonist[4,5] demonstrating that specific binding of [^{11}C]doxepin in the cerebellum is negligibly small. In addition, postmortem human studies revealed that the H1R density in the cerebellum was less than a tenth of that in the frontal cortex.[20,25] Thus, it appears that the first assumption is justified in the present case.

The second assumption states that K_1/k_2 should be equal in the target and reference tissues. It is impossible to directly prove that K_1/k_2 is equal in all the brain regions in the case of [^{11}C]doxepin since K_1, k_2, k_3 and k_4 were not available with 2TM.[12] However, a previous study demonstrated a similar amount of nonspecific binding in the cerebellum and cerebral cortices.[25] Thus the second assumption holds for the cortical tissues, and it appears to justify calculation of *BP* values with LGAR.

Furthermore, the excellent correlation between *BP* values estimated by LGAR and 1TM ($r = 0.96$: $p < 0.001$) justifies the use of the cerebellar ROI value as a reference input. The failure rates, one of the criteria for validation of these modeling methods, were 1.2%, 2.4% and 0% for LGAR, LGA and 1TM, respectively. Because the graphical analysis requires no apriori choice of compartment configuration, the correlation to *DV* values calculated by LGA is a possible criterion for choosing a compartment configuration.

The noise simulation demonstrated that 1TM provided better parameter estimation than LGA in the presence of noise (Fig. 4). In addition, the failure rate of 1TM was 0% and the correlation between *BP* with 1TM and biopsy data in the cortical regions was strong ($r = 0.93$). As described previously, 1TM described [^{11}C]doxepin kinetics better than 2TM.[12] Therefore, we chose 1TM as the reference in the present study. Comparison between H1R densities and *BP* values from LGAR, LGA and 1TM showed much better correlations in the cortical regions than in other brain regions. One of the reasons to explain this might be relatively high nonspecific binding in these regions.[25] Therefore, the parameters in the regions with high nonspecific binding should be evaluated with caution. On the other hand, since specific binding in the cortex is relatively high, *BP* estimation in the cortex is more reliable.

In the simulations to evaluate stability to noise, the bias of *BP* values from LGAR is larger than those obtained from LGA and 1TM at all noise levels. To determine the noise level corresponding to the noise level in actual brain image data, we compared the mean sum of squares of residuals in simulation data at each noise level to the ones of the actual image datasets. For *BP* estimation in the temporal cortex with LGAR, this comparison revealed that the noise level of actual brain image data corresponds to a noise level of 10 to 15 (Fig. 4) resulting in average bias of –2.2% to –2.8%. On the other hand, for *BP* estimation in the occipital cortex with LGAR, the noise level of actual brain image data corresponded to noise levels of 10 to 15 resulting here in average bias of –3.1% to –3.7%. These results suggest that reliable parameter estimation with small bias is provided by LGAR as long as the noise level of actual brain data remains around 10 to 15 in the cortex, although LGAR underestimates the true values, when the noise level of actual brain data is higher, as mentioned already.[26]

In summary, in the present study, we analyzed [^{11}C]doxepin binding with SRTM, LGAR, LGA and 1TM. Comparison of *BP* values estimated by LGAR showed an excellent correlation with 1TM. On the other hand, SRTM did not provide satisfactory parameter estimation in several brain regions. At the noise level of actual brain data, LGAR was able to provide reliable parameter estimation in the cortex with small bias. Since LGAR does not require arterial blood sampling, this method is a useful tool for clinical studies for H1R quantification with PET and [^{11}C]doxepin. This method can be applied to investigation of brain H1R densities in various physiological and pharmacological conditions in healthy and diseased subjects in the near future, although the present study used only a limited number of normal subjects ($n = 5$). We expect a growing number of nuclear medicine techniques will be applied in related fields using convenient methods as discussed in this paper.

ACKNOWLEDGMENTS

This work was partly supported by Grants-in-Aid from the Ministry of Education, Culture, Sports, Science, and Technology, and from the Ministry of Health, Labor and Welfare, Japan. The authors thank the volunteers in the PET measurement, Keiichi Oda, Ph.D. and Ms. Miyoko Ando for their help in PET measurements and Toru Sasaki, Ph.D. and Kazunori Kawamura, Ph.D. for the preparation of [^{11}C]doxepin. The authors also thank Professor Masatoshi Itoh, at Tohoku University Cyclotron and Radioisotope Center, for his valuable comments and advice.

REFERENCES

1. Haas H, Panula P. The role of histamine and the tuberomamillary nucleus in the nervous system. *Nat Rev Neurosci* 2003; 4 (2): 121–130.
2. Yanai K, Okamura N, Tagawa M, Itoh M, Watanabe T. New findings in pharmacological effects induced by antihista-

mines: from PET studies to knock-out mice. *Clin Exp Allergy* 1999; 29 Suppl 3: 29–36; discussion 37–38.
3. Huang ZL, Qu WM, Li WD, Mochizuki T, Eguchi N, Watanabe T, et al. Arousal effect of orexin A depends on activation of the histaminergic system. *Proc Natl Acad Sci USA* 2001; 98 (17): 9965–9970.
4. Yanai K, Watanabe T, Yokoyama H, Meguro K, Hatazawa J, Itoh M, et al. Histamine H_1 receptors in human brain visualized *in vivo* by [^{11}C]doxepin and positron emission tomography. *Neurosci Lett* 1992; 137 (2): 145–148.
5. Ishiwata K, Kawamura K, Wang WF, Tsukada H, Harada N, Mochizuki H, et al. Evaluation of *in vivo* selective binding of [^{11}C]doxepin to histamine H_1 receptors in five animal species. *Nucl Med Biol* 2004; 31 (4): 493–502.
6. Higuchi M, Yanai K, Okamura N, Meguro K, Arai H, Itoh M, et al. Histamine H(1) receptors in patients with Alzheimer's disease assessed by positron emission tomography. *Neuroscience* 2000; 99 (4): 721–729.
7. Iinuma K, Yokoyama H, Otsuki T, Yanai K, Watanabe T, Ido T, et al. Histamine H_1 receptors in complex partial seizures. *Lancet* 1993; 341 (8839): 238.
8. Yanai K, Ryu JH, Watanabe T, Iwata R, Ido T, Sawai Y, et al. Histamine H_1 receptor occupancy in human brains after single oral doses of histamine H_1 antagonists measured by positron emission tomography. *Br J Pharmacol* 1995; 116 (1): 1649–1655.
9. Tagawa M, Kano M, Okamura N, Higuchi M, Matsuda M, Mizuki Y, et al. Neuroimaging of histamine H_1-receptor occupancy in human brain by positron emission tomography (PET): a comparative study of ebastine, a second-generation antihistamine, and (+)-chlorpheniramine, a classical antihistamine. *Br J Clin Pharmacol* 2001; 52 (5): 501–509.
10. Tashiro M, Sakurada Y, Iwabuchi K, Mochizuki H, Kato M, Aoki M, et al. Central Effects of Fexofenadine and Cetirizine: Measurement of Psychomotor Performance, Subjective Sleepiness, and Brain Histamine H_1-Receptor Occupancy Using ^{11}C-Doxepin Positron Emission Tomography. *J Clin Pharmacol* 2004; 44 (8): 890–900.
11. Logan J, Fowler JS, Volkow ND, Wolf AP, Dewey SL, Schlyer DJ, et al. Graphical analysis of reversible radioligand binding from time-activity measurements applied to [*N*-^{11}C-methyl]-(–)-cocaine PET studies in human subjects. *J Cereb Blood Flow Metab* 1990; 10 (5): 740–747.
12. Mochizuki H, Kimura Y, Ishii K, Oda K, Sasaki T, Tashiro M, et al. Quantitative measurement of histamine H(1) receptors in human brains by PET and [^{11}C]doxepin. *Nucl Med Biol* 2004; 31 (2): 165–171.
13. Mochizuki H, Kimura Y, Ishii K, Oda K, Sasaki T, Tashiro M, et al. Simplified PET measurement for evaluating histamine H_1 receptors in human brains using [^{11}C]doxepin. *Nucl Med Biol* (in press).
14. Lammertsma AA, Hume SP. Simplified reference tissue model for PET receptor studies. *Neuroimage* 1996; 4 (3 Pt 1): 153–158.
15. Logan J, Fowler JS, Volkow ND, Wang GJ, Ding YS, Alexoff DL. Distribution volume ratios without blood sampling from graphical analysis of PET data. *J Cereb Blood Flow Metab* 1996; 16 (5): 834–840.
16. Mintun MA, Raichle ME, Kilbourn MR, Wooten GF, Welch MJ. A quantitative model for the *in vivo* assessment of drug binding sites with positron emission tomography. *Ann Neurol* 1984; 15 (3): 217–227.
17. Koeppe RA, Holthoff VA, Frey KA, Kilbourn MR, Kuhl DE. Compartmental analysis of [^{11}C]flumazenil kinetics for the estimation of ligand transport rate and receptor distribution using positron emission tomography. *J Cereb Blood Flow Metab* 1991; 11 (5): 735–744.
18. Phelps ME, Huang SC, Hoffman EJ, Kuhl DE. Validation of tomographic measurement of cerebral blood volume with C-11-labeled carboxyhemoglobin. *J Nucl Med* 1979; 20 (4): 328–334.
19. Carson RE, Parameters estimation in positron emission tomography. In: *Positron emission tomography. Principles and applications for the brain and the heart*. Phelps ME, Mazziotta JC, Schelbert HR (eds). New York; Raven Press, 1986: 347–390.
20. Kanba S, Richelson E. Histamine H_1 receptors in human brain labelled with [^{3}H]doxepin. *Brain Res* 1984; 304 (1): 1–7.
21. Kimura Y, Senda M, Alpert NM. Fast formation of statistically reliable FDG parametric images based on clustering and principal components. *Phys Med Biol* 2002; 47 (3): 455–468.
22. Gunn RN, Lammertsma AA, Hume SP, Cunningham VJ. Parametric imaging of ligand-receptor binding in PET using a simplified reference region model. *Neuroimage* 1997; 6 (4): 279–287.
23. Jensen SB, Smith DF, Bender D, Jakobsen S, Peters D, Nielsen EO. [^{11}C]-NS 4194 versus [^{11}C]-DASB for PET imaging of serotonin transporters in living porcine brain. *Synapse* 2003; 49: 170–177.
24. Sossi V, Holden JE, Chan G, Krzywinski M, Stoessl AJ, Ruth TJ. Analysis of four dopaminergic tracers kinetics using two different tissue input function methods. *J Cereb Blood Flow Metab* 2000; 20 (4): 653–660.
25. Yanai K, Watanabe T, Meguro K, Yokoyama H, Sato I, Sasano H, et al. Age-dependent decrease in histamine H_1 receptor in human brains revealed by PET. *Neuroreport* 1992; 3 (5): 433–436.
26. Logan J, Fowler JS, Ding YS, Franceschi D, Wang GJ, Volkow ND, et al. Strategy for the formation of parametric images under conditions of low injected radioactivity applied to PET studies with the irreversible monoamine oxidase A tracers [^{11}C]clorgyline and deuterium-substituted [^{11}C]clorgyline. *J Cereb Blood Flow Metab* 2002; 22 (11): 1367–1376.